X-RAY DIFFRACTION ANALYSIS OF BARTON OXIDES

A. de la TORRE, M. TORRALBA, A, GARCÍA and P. ADEVA

Centro Nacional de Investigaciones Metalúrgicas, C.S.I.C., Avda, de Gregorio del Amo, 8. 28040 Madrid (Spain)

(Received October 9, 1984)

Summary

In consequence of the influence of the composition of Barton oxides on the behaviour of batteries, a method has been developed for the quantitative determination of orthorhombic and tetragonal monoxides.

An X-ray diffraction, internal standard method was used. Factors such as diffraction peak overlapping and its method of measurement, type of radiation, particle size as a function of the mass absorption coefficient, and the wavelength used, were all taken into account.

An operational method was established and a statistical error analysis was carried out. Although the error varies with both chemical species and concentration, it can be considered as acceptable.

Introduction

In a very simplified form, it may be considered that lead–acid batteries consist of a series of lead grids, impregnated with "so-called" active material, some of which are positive electrodes and others negative electrodes immersed in dilute sulphuric acid.

Preparation of the active material is carried out in several steps:

(a) preparation of lead monoxides;
(b) pasting;
(c) curing;
(d) forming the active material.

Preparation of lead monoxides

Lead monoxides may be obtained in several ways — typically by the oxidation of lead in a ball mill or, more frequently, by the Barton procedure. This consists of partially oxidizing molten lead by bubbling air through it. The lead monoxide obtained by this process is present in its two allotropic forms: orthorhombic and tetragonal [1]. In addition, a significant amount of unoxidized lead is also obtained as well as, occasionally, a trace of red lead [2]. Temperature, stirring rate of air, and lead flow would also influence the amount of lead monoxide obtained.

0378-7753/85/$3.30

Pasting

The starting powder material is mixed with sulphuric acid and water, and the mixture is used to paste the grids. Several complex chemical reactions, which take place during this operation, give rise to the formation of Pb, PbO, $PbSO_4$, Pb_3O_4, $PbO \cdot PbSO_4$, $3PbO \cdot H_2O \cdot PbSO_4$(tribasic lead sulphate) and $4PbO \cdot PbSO_4$(tetrabasic lead sulphate). The exact composition depends on several factors, but the main constituents are lead monoxides and sulphates [3, 4].

Curing

This operation consists of leaving the paste to dry in a moist and warm atmosphere when new chemical reactions take place. Generally speaking, the substances are the same, but their relative amounts can vary significantly depending on temperature and humidity conditions [2].

Formation of active materials

After curing, the plates are immersed in H_2SO_4 and "formed" by passing a current to create the active materials. This current flow reduces the paste to a spongelike mass of Pb in the negative plate, and results in oxidation to lead dioxide in the positive plate. The battery is thus ready for operation.

The following reactions take place during normal operation:

(a) In the negative electrode:

$$Pb + SO_4^{2-} \underset{\text{charge}}{\overset{\text{discharge}}{\rightleftharpoons}} PbSO_4 + 2e^-$$

(b) In the positive electrode:

$$PbO_2 + 4H^+ + SO_4^{2-} + 2e^- \underset{\text{charge}}{\overset{\text{discharge}}{\rightleftharpoons}} PbSO_4 + 2H_2O$$

Altogether, the overall reaction which takes place in the battery is:

$$Pb + PbO_2 + 2H_2SO_4 \underset{\text{charge}}{\overset{\text{discharge}}{\rightleftharpoons}} 2PbSO_4 + 2H_2O$$

The characteristics of the battery are influenced by the relative amounts of elements present in the active material. These, in turn, depend on acid concentration, temperature, humidity, etc., during the pasting, curing, and formation of active material, and on the composition of starting materials [5].

Thus, mill oxides contain only tetragonal PbO, whereas thermal oxides (Barton type) are predominantly tetragonal but with some orthorhombic PbO (up to about 15% by weight). If tetrabasic sulphate, $4PbO \cdot PbSO_4$, is desired in the paste, orthorhombic-rich oxides would be used, while the formation of tribasic sulphate, $3PbO \cdot H_2O \cdot PbSO_4$, is favoured by the presence of tetragonal PbO. At temperatures below 80 °C a large amount of $3PbO \cdot H_2O \cdot PbSO_4$ is present [3]; however, some authors report that plates

cured at higher temperatures darken considerably: the phenomenon is related to an increase in the amount of tetrabasic sulphate formed from the tribasic variety [2]. At these high temperatures the $3PbO \cdot H_2O \cdot PbSO_4$ reacts with the tetragonal PbO giving rise to $4PbO \cdot PbSO_4$. This reaction, however, takes place only in the presence of orthorhombic PbO [3].

From the above discussion it may be concluded that a determination of the relative amounts of the lead monoxides present is a basic preliminary step in the control of the manufacturing process.

Chemical methods are generally unsuitable for the determination of the allotropic chemical species and, hence, quantitative X-ray diffraction analysis should be used [6].

Quantitative analysis by diffraction is based on the fact that the intensity of the diffraction pattern of a particular phase in a mixture of phases depends on the concentration of that phase in the mixture [7]. This relationship between intensity and concentration is not usually linear, since intensity varies with the absorption coefficient of the mixture and this varies with the concentration.

In this work an internal standard method was used [7 - 9]. It is based on the fact that if one phase in a compound is a constant percentage of the total mass then the ratio between the intensities of the X-ray diffraction peaks of this (reference) phase and those of a phase whose mass is unknown is a linear function of the mass percentage of this unknown phase, regardless of the remaining phases in the sample. Calibration was achieved by measuring the intensities of the two phases in a group of standard synthetic samples. These were prepared by mixing various amounts of the problem phase with constant amounts of a phase chosen as standard, a third phase being added to keep the total constant. The determination of the peak intensity ratio of the problem phase peak was sufficient to plot the calibration line.

The microabsorption and extinction effects, should they exist, can be minimized by the internal standard method since such effects are constant in all the samples, including the standard samples. Care must be taken in sample preparation, however, in order to avoid preferred orientations since this could lead to erroneous intensity measurements.

Experimental

(i) Problem substances

As stated in the Introduction, each allotropic form of PbO, tetragonal and orthorhombic, as well as pure lead, was analyzed.

Tetragonal red lead monoxide is stable at low temperature with lattice parameters: $a = 3.976$ Å and $b = 5.023$ Å. Each lead atom has four adjacent oxygen atoms in the form of a pyramid with a Pb–O spacing of 2.33 Å. The structure is a distortion of the cubic packing due to the incorporation of oxygen atoms [4].

The second form of lead monoxide is the high-temperature-equilibrium yellow phase, which is orthorhombic with lattice parameters: a = 5.891 Å, b = 4.775 Å, and c = 5.489 Å. It is layered perpendicular to the "z" axis and, in each layer, the lead atom is surrounded by 4 oxygen atoms to form a pyramid. There are four PbO molecules in each crystalline cell. Orthorhombic lead monoxide is obtained by heating the lead carbonate to about 700 °C. Tetragonal lead monoxide is obtained by heating the lead carbonate to temperatures between 350 and 500 °C [10].

Little is known about the allotropic transformation of lead monoxide, except that there is a transformation point between each phase at 488.5 °C, at atmospheric pressure. Tetragonal, red t-PbO is stable below this temperature, while yellow o-PbO is stable above it [11].

On heating the tetragonal form to above the allotropic temperature it is possible to observe transformation to the orthorhombic form. On the other hand, when the orthorhombic form cools, the inverse reaction only takes place at an extremely low rate. As a result, the tetragonal and orthorhombic forms co-exist at room temperature.

By mechanical grinding, the orthorhombic form [12] tends to transform into the tetragonal form, provided that it is carried out below 488.5 °C.

Lead has a face-centred cubic structure with a lattice parameter of 4.950 Å.

(ii) Choice of standard and ballast

The preparation of standard synthetic samples requires the selection of two other crystalline substances in addition to o-PbO, t-PbO and Pb. One is the standard and the other is the ballast to keep the sample mass constant while keeping pre-established ratios between the unknown and the standard. These two substances must meet certain requirements. Both must have a diffraction pattern whose lines do not interfere with those of the unknown, at least for the peaks to be measured, which must either be those of maximum intensity or those with a high peak-to-background-noise ratio, thus making for an acceptable measurement error. It is also necessary for the standard to be a material which is not normally found in any of the samples so that it can be included in precisely determined amounts (20% of the mass of the complete specimen in our case or 25% of standard added to the problem specimen). As for the ballast, it is sufficient for its diffraction peaks not to interfere with those of the standard and the unknown. The diffraction patterns must therefore be determined for all components so that these requirements are met.

After taking into account data from the literature [13], diffraction patterns of the problem substances were obtained, and it was found that the most important peaks are those given in Tables 1 - 3.

Once such data were known, the Powder Diffraction File [13] was searched for easily available substances which would meet the requirements. Calcium fluoride was chosen as the standard and nickel as ballast, taking into consideration the influence of preferred orientations and absorption

TABLE 1

Diffraction maxima o-PbO (File No. 5-570 [13])

Lattice spacing, d (Å)	Relative intensity, I	Angle (2θ) for Cu Kα radiation
3.07	10	20.09
2.95	3	30.30
2.74	2	32.68
2.38	2	37.80
1.71	1	53.59
1.85	1	49.26

TABLE 2

Diffraction maxima t-PbO (File No. 5-561 [13])

Lattice spacing, d (Å)	Relative intensity, I	Angle (2θ) for Cu Kα radiation
3.12	10	28.61
2.81	6	31.84
1.87	3	48.69
1.68	2	54.63
2.51	1	35.77
1.54	1	60.08

TABLE 3

Diffraction maxima Pb (File No. 4-686 [13])

Lattice spacing, d (Å)	Relative intensity, I	Angle (2θ) for Cu Kα radiation
2.86	10	31.28
2.48	5	36.22
1.49	3	62.32
1.75	3	52.28
1.14	1	85.10
1.43	0	62.25

TABLE 4

Diffraction maxima CaF_2 (File No. 4-864 [13])

Lattice spacing, d (Å)	Relative intensity, I	Angle (2θ) for Cu Kα radiation
1.93	10	47.09
3.15	9	28.33
1.65	3	55.70
1.12	1	87.01
1.37	1	68.50
1.25	1	76.16

TABLE 5

Diffraction maxima Ni (File No. 4-850 [13])

Lattice spacing, d (Å)	Relative intensity, I	Angle (2θ) for Cu Kα radiation
2.03	10	44.64
1.76	4	51.96
1.25	2	76.16
1.06	2	93.33
0.79	1	154.82
0.81	1	144.30

coefficients on the appearance, which will be discussed later. Tables 4 and 5 give spacings and intensities for these substances arranged in decreasing order of intensities.

As can be seen, considerable difficulties arise. Maximum intensity peaks of o-PbO and t-PbO practically overlap, as the plane families which gave rise to them have very similar interplanar spacings, namely, 3.07 Å and 3.12 Å, and thus they could not be used. For this reason it was necessary to resort to other diffraction maxima of lower intensity, corresponding to plane families with interplanar spacings of 2.99 Å and 2.81 Å. Nevertheless, the peak for the 2.81 Å family almost overlaps that of lead with an interplanar spacing d = 2.86 Å. The reason for using this plane family was that the following one for t-PbO, with an interplanar spacing of 1.87 Å, is too weak. The intensity ratio for the d = 2.95 Å in o-PbO, compared with the maximum peak for artificial alumina (corundum), is 2.2, while for d = 2.81 Å it is reduced to 1.26 and for 1.87 Å to only 0.63, thus producing unacceptable errors. In addition, this line overlaps the peak for d = 1.85 Å of o-PbO. This was the first compromise that had to be accepted.

To determine the amount of Pb in the sample the plane family with an interplanar spacing of 1.49 Å was chosen. This was because, as already stated, the most intense line (d = 2.86 Å) overlaps that for d = 2.81 Å of t-PbO, while the second line in order of intensity (d = 2.48 Å) overlaps the third most intense line of o-PbO (d = 2.38 Å).

No problems arose in the case of the calcium fluoride reference material. The maximum intensity line (d = 1.93 Å) does not overlap any of the lines of the problem substances since, although that from 1.85 Å of o-PbO is close, its perfect crystallisation gives rise to a very sharp maximum. The remaining peaks do not interfere with any of the lines on which determinations were to be made. Nickel does not present problems of this type.

In addition to its good crystallisation and low mass absorption coefficient, calcium fluoride also contributes to the removal of preferred orientations. This is of particular interest when such compounds as o-PbO are present since they have a marked tendency to become oriented in preferred planes or directions [14].

(iii) Sample preparation

Figure 1 shows a diffraction pattern for a sample whose composition is 15% o-PbO, 22.5% t-PbO, 50% Pb and 12.5% Ni, which has been blended with a constant amount of 25% of reference material (CaF_2). The sample was homogenized for 60 min in a ball mill. A rotating sample holder and a 1° scatter slit were used, with Cu as the target and an LiF single-crystal, curved monochromator. The scanning rate was 2° (2θ)/min. The main difficulty lay in the integration of the t-PbO maximum, corresponding to a 2.81 Å interplanar spacing.

To obtain good reproducibility, compromises had to be made as there were several factors which interact. The most important were: particle size, chemical homogeneity in samples, freedom from preferred orientations and a suitable and well-monochromized radiation wavelength.

In general, a very fine particle size is required. Thus, in a stationary test specimen the crystallite size should not be greater than 5 μm when μ^+, the

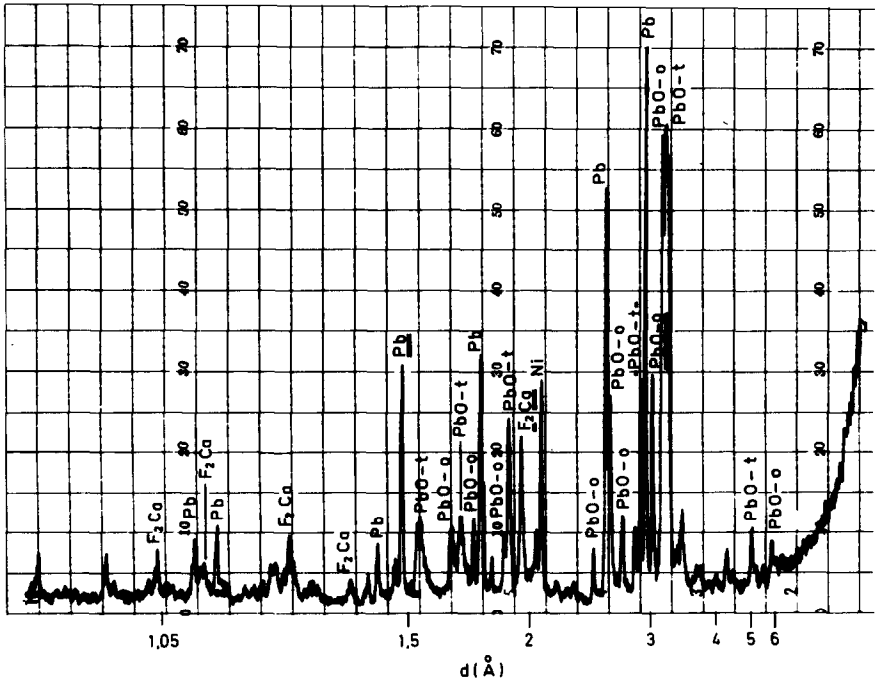

Fig. 1. Diffraction pattern for synthetic sample.

mass absorption coefficient, is of the order of 40 cm^2/g, while for higher μ^+ values the crystallite size should be smaller. In our case, as will be seen later, when operating with Cu Kα radiation, μ^+ has values of about 200 cm^2/g and therefore our crystallite size should be well under 5 μm. Particles may contain several crystallites, however, and this is not readily known, and for that reason the particle size should be below 5 μm. This size may be increased somewhat, however, perhaps two or three fold, if a rotary sample-holder is used which also reduces measurement errors caused by preferred orientations.

On the other hand, Bridley [15] proposed that the maximum particle size should be of the order of $1/100\ \bar{\mu}$, where $\bar{\mu}$ is the linear absorption coefficient due to microabsorption. In our case that would mean $1/100 \times 1600\ cm^{-1}$ or 0.06 microns, a size impossible to obtain because, among other reasons, on every particle obtained by grinding there is a very thin, amorphous layer which dominates the characteristics of very fine particles. Therefore, we had to operate with particle sizes higher than the optimum.

Mention has also been made of the significance of chemical homogeneity. This is obtained by grinding for a sufficiently long time in a ball mill which simultaneously reduces the grain size and encourages homogeneity. In our case, some synthetic samples of known composition were prepared using the materials mentioned earlier, Table 6.

TABLE 6

Chemical composition* of 17 synthetic samples, mass %

Sample no.	Ballast Ni	o-PbO	t-PbO	Pb
M-1	—	12.50	82.50	5.00
M-2	5.00	35.00	30.00	30.00
M-3	5.00	25.00	62.50	7.50
M-4	12.50	15.00	22.50	50.00
M-5	12.50	30.00	37.50	20.00
M-6	6.25	6.25	50.00	37.50
M-7	1.25	18.75	75.00	5.00
M-8	12.50	43.75	43.75	—
M-9	5.00	22.50	57.50	15.00
M-10	2.50	60.00	25.00	12.50
M-11	12.50	37.50	17.50	32.50
M-12	2.50	50.00	12.50	35.00
M-13	5.00	17.50	60.00	17.50
M-14	10.00	32.50	32.50	25.00
M-15	—	100.00	—	—
M-16	5.00	85.00	10.00	—
M-17	—	77.50	22.50	—

*25% CaF_2 was subsequently added to each synthetic sample to complete the sample used for calibration.

The optimum milling time was studied with a view to avoiding the transformation of o-PbO to t-PbO [16] which can take place if the times are prolonged. Mixed samples and samples of pure orthorhombic lead monoxide, o-PbO, were subjected to 10, 20, 30, 40, 50 and 60 min of milling. The diffraction patterns were then used to determine the degree of homogeneity of the first set of samples, and whether transformation of o-PbO to t-PbO had taken place in the second set.

Sixty minutes gave homogeneous samples without transforming the o-PbO to t-PbO.

To avoid, as much as possible, the production of preferred orientations in the samples, they were prepared by the method suggested by Alexander and Klug [17]. The edge of a spatula was used to work the powder in a perpendicular direction to the surface of the sample before it was compacted.

The average particle size obtained was 3.50 μm with a variation coefficient of 83% [18].

The powder was compacted in a press without the addition of binder or agglomerant, which might alter the values obtained.

(iv) Diffractometer conditions

A curved, LiF single crystal was used to obtain monochromatic radiation and a pulse height discriminator improved the signal/background noise ratio.

TABLE 7

Substance	Lattice spacing, d (Å)	Angle (2θ) for Ag Kα radiation	Angle (2θ) for Cu Kα radiation
o-PbO	2.95	11.50	30.30
t-PbO	2.81	12.07	31.84
Pb	1.49	22.87	62.32
CaF_2	1.93	17.61	47.09

The operating conditions were as follows:
— A copper target with characteristic radiation. Kα = 1.542 Å.
— A 1° divergence slit.
— A 1° receiving slit.
— 0.2 mm sample thickness.
— Voltage setting 40 kV.
— Intensity 20 mA.
The plane families for which diffraction was studied were [19, 20]:
— For o-PbO, plane (200) corresponding to a value of $2\theta = 30.30°$.
— For t-PbO, plane (110) corresponding to a value of $2\theta = 31.84°$.
— For Pb, plane (311) corresponding to a value of $2\theta = 62.32°$.
— For CaF_2, plane (220) corresponding to a value of $2\theta = 47.09°$.

In the case of a typical mixture (o-PbO 22.5%, t-PbO 57.5%, Pb 15%, Ni 5%, and CaF_2 25%) the mass absorption coefficient of the sample would be, for Cu Kα radiation (λ = 1.542 Å), $\mu^+ = 192$ cm^2 g^{-1}, and given that density is 8.27 g cm^{-3}, the linear absorption coefficient is $\bar{\mu} = 1588$ cm^{-1}, which leads to a maximum particle size of $t_{max} = 0.06$ μm as commented upon earlier.

Since this is an extremely small size, a smaller wavelength was considered to enable a large particle size to be employed. This requirement can be met by an Ag target. In this case, given that Kα = 0.5909 Å, the mass absorption coefficient takes the value of $\mu^+ = 51.59$ cm^{-2} g^{-1} and the linear absorption coefficient takes the value $\bar{\mu} = 426$ cm^{-1}. Consequently, $t_{max} = 0.235$ μm.

From this viewpoint, silver is better than copper, but there are disadvantages which make it unsuitable. The diffraction peaks are closer, so they are more difficult to discriminate as shown in Table 7. Furthermore, the peak/background ratio becomes impaired.

Table 7 shows that the difference between the 2θ values for the o-PbO and t-PbO peaks is 0.57 for silver while it is 1.54 for copper, and therefore the latter was chosen.

(v) Intensity measurements

There are four methods for measuring the diffracted intensity [21]:

— Peak height.
— Height of peak at half-peak width.
— Step integration.
— Continuous integration.

The step integration method is the most precise but it was difficult to apply in the present case due to the unavoidable overlapping of the diffraction peaks. It was therefore necessary to resort to another method provided that the errors introduced were not excessive. A measurement of peak height is not to be recommended for quantitative analysis except in very simple cases, due to the errors introduced, so it was discarded. The continuous integration method was also discarded since it posed the same problems as the step integration technique with no additional advantage other than greater speed. Therefore, only the "height of peak at half-peak width" method remained. To ensure that the errors introduced into the analysis were not much greater than if the step integration method were used, measurements obtained by both methods were compared.

To this end, ten t-PbO sample holders, designated A-1, A-2, A-3, ... A-10 were prepared. The intensity ratio I_1/I_2 was measured in every peak corresponding to the interplanar spacings d_1 = 3.12 Å and d_2 = 2.81 Å by the following procedures:

Method I: height of peak at half-peak width.
Method II: step peak integration.
Ratios I_1/I_2 obtained by both methods are given in Table 8.

TABLE 8

Intensity ratios obtained by Method I and Method II

	A-1	A-2	A-3	A-4	A-5	A-6	A-7	A-8	A-9	A-10
I	5.325	4.965	5.009	4.913	5.064	5.023	4.878	5.029	5.301	4.959
II	5.245	5.345	5.085	5.007	5.315	5.114	5.117	5.197	5.545	5.064

Mean $\bar{X}$ and standard deviation, S, for each method are:

Method I $\quad \bar{X}_I = 5.047 \quad S_I = 0.152$
Method II $\quad \bar{X}_{II} = 5.203 \quad S_{II} = 0.163.$

To estimate the distribution average, Student's "t" Tables were used for a 98% confidence level and $n - 1 = 9$ degrees of freedom [22] which implies a confidence coefficient $(t_9)_{0.02} = \pm 2.821$.

The estimate of the mean μ is given by:

$$\mu = \bar{X} \pm t_{n-1} \frac{S}{(n)^{1/2}}$$

By calculating the error in the mean value for each of the two methods of measurement of the diffracted intensity, one gets

Method I $\mu_I = 5.047 \pm 0.135$

Method II $\mu_{II} = 5.203 \pm 0.145$

To compare method I with method II, the difference in mean distribution was developed in order to determine its magnitude. The difference in mean distribution for average values is given by equation

$$\mu_I - \mu_{II} = (\bar{X}_I - \bar{X}_{II}) \pm (t_{n_1+n_2-2})\left[\left(\frac{(n_1-1)S_I^2 + (n_2-1)S_{II}^2}{n_I + n_{II} - 2}\right)\left(\frac{1}{n_I} + \frac{1}{n_{II}}\right)\right]^{1/2} \quad (1)$$

where n_I and n_{II} are the number of measurements undertaken by each method. In our case $n_I = n_{II} = 10$.

The distribution of the mean value difference is thus given by

$$\mu_I - \mu_{II} = -0.156 \pm 0.179$$

since $(t_{18})_{0.02} = \pm 2.552$.

The accuracy of the foregoing estimations was then verified. To this end the "t" or "nil" hypothesis test was undertaken, where $\mu_I - \mu_{II} = 0$. t-Student was calculated from eqn. (1)

$$t = -\frac{0.156}{0.070} = -2.213$$

this value for t is within the confidence range as it is smaller than $(t_{18})_{0.02} = \pm 2.552$, and the difference between the average values obtained is not significant for a 98% confidence level.

As the differences were not significant, it was considered that method I should be chosen in preference to method II, without there being any great risk of obtaining considerably different results. Furthermore, to obtain greater accuracy and to avoid possible accidental errors, each sample was measured three times and the mean value used.

Results

Table 6 gives the compositions of 17 samples artificially prepared to determine the calibration curves, that is, to establish a relationship between the diffracted intensity by 25% calcium fluoride and different amounts of o-PbO, t-PbO and Pb.

The experimental results are given in Tables 9 - 11 for o-PbO, t-PbO, and Pb, respectively. Table 9 provides the intensity ratio between peaks $d = 2.95$ Å of orthorhombic lead monoxide and $d = 1.93$ Å for calcium fluoride. Table 10 shows the relationship between peaks $d = 2.81$ Å for tetragonal lead monoxide and $d = 1.93$ Å for calcium fluoride, while Table 11 refers to the relationship between peaks $d = 1.49$ Å for lead and $d = 1.93$ Å for calcium fluoride.

TABLE 9

Diffracted intensity ratio for o-PbO and CaF_2

Sample	o-PbO (%)	$I_{o\text{-}PbO}/I_{CaF_2}$
M-1	12.50	1.71
M-2	35.00	5.57
M-3	25.00	3.14
M-4	15.00	2.03
M-5	30.00	4.56
M-6	6.25	0.69
M-7	18.75	2.55
M-8	43.75	7.02
M-9	22.50	2.65
M-10	60.00	9.27
M-11	37.50	5.34
M-12	50.00	8.14
M-13	17.50	2.33
M-14	32.50	5.01
M-15	100.00	17.81
M-16	85.00	14.28
M-17	77.50	13.07

TABLE 10

Diffracted intensity ratio for t-PbO

Sample	t-PbO (%)	$I_{t\text{-}PbO}/I_{CaF_2}$
M-1	82.50	3.26
M-2	30.00	1.29
M-3	62.50	2.65
M-4	22.50	0.98
M-5	37.50	1.81
M-6	50.00	1.86
M-7	75.00	3.12
M-8	43.75	1.43
M-9	57.50	2.60
M-10	25.00	0.93
M-11	17.50	0.75
M-12	12.50	0.62
M-13	60.00	2.33
M-14	32.50	1.34
M-15	—	—
M-16	10.00	0.60
M-17	22.50	0.74

TABLE 11

Diffraction intensity for Pb

Sample	Pb (%)	I_{Pb}/I_{CaF_2}
M-1	5.00	0.09
M-2	30.00	0.72
M-3	7.50	0.10
M-4	50.00	1.13
M-5	20.00	0.40
M-6	37.50	1.00
M-7	5.00	0.08
M-8	—	—
M-9	15.00	0.23
M-10	12.50	0.20
M-11	32.50	0.57
M-12	35.00	0.71
M-13	17.50	0.30
M-14	25.00	0.44
M-15	—	—
M-16	—	—
M-17	—	—

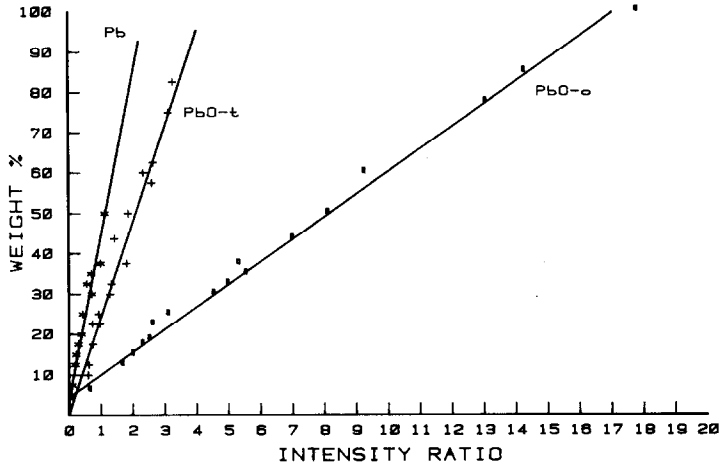

Fig. 2. Calibration lines for o-PbO, t-PbO and Pb using fluorite as internal standard.

These results are shown in graphic form in Fig. 2. The lines were obtained by the least squares method, including the origin as one of the points.

The equations obtained for these lines are:

	Line equation	Correlation coefficient	Sample variance about regression
o-PbO	$y = 4.540 + 5.582x$	0.996	5.5
t-PbO	$y = 0.373 + 23.894x$	0.981	17.9
Pb	$y = 3.732 + 40.391x$	0.976	11.05

As an example, two Barton oxides of unknown composition and supplied by a battery manufacturer were analyzed.

The oxides were subjected to the same process as the synthetic samples, that is, they were mixed with 25% CaF_2 and homogenized for 60 min. At the same time, three specimens per sample were examined.

The intensity ratios obtained were as follows:

	$I_{o\text{-}PbO}/I_{CaF_2}$	$I_{t\text{-}PbO}/I_{CaF_2}$	I_{Pb}/I_{CaF_2}
1-Barton	1.07	3.83	—
2-Barton	8.51	1.12	0.27

When compared with the corresponding calibration lines, we get the following concentrations in mass percent:

	o-PbO	t-PbO	Pb	Total
1-Barton	10.5	92.0	—	102.5
2-Barton	52.1	27.1	14.6	93.8

Since these concentrations are only an estimate of real value, we consider it appropriate to give an idea of the confidence range.

In any regression line, the difference between the estimated value and the real mean value for a given X_0 value of the depending variable is distributed according to a t-Student with $n - 2$ freedom degrees, so that

$$P[E|\hat{y}| - t_{n-2} \cdot S_{\hat{y}} \leqslant E|y| \leqslant E|\hat{y}| + t_{n-2} \cdot S_{\hat{y}}] = 1 - \alpha$$

where:

$E|\hat{y}|$ is the estimated value of the depending variable for a given X_0

$$S_{\hat{y}}^2 = S_{ry}^2 \left(\frac{1}{n} + \frac{(x_0 - \bar{x})^2}{\Sigma (x_i - \bar{x})^2} \right)$$

S_{ry}^2 is the sample variance about regression.

n is the number of points used for the regression calculation.

$(1 - \alpha) \cdot 100$ is the confidence estimate.

The confidence ranges thus calculated for each chemical species which make up the Barton oxides studied, for a 95% confidence level, are as follows:

1-Barton

$P[8.9 \leqslant \%\ \text{o-PbO} \leqslant 12.1] = 0.95$

$P[86.1 \leqslant \%\ \text{t-PbO} \leqslant 97.7] = 0.95$

2-Barton

$P[50.8 \leqslant \%\ \text{o-PbO} \leqslant 53.4] = 0.95$

$P[24.7 \leqslant \%\ \text{t-PbO} \leqslant 29.5] = 0.95$

$P[12.5 \leqslant \%\ \text{Pb} \leqslant 16.7] = 0.95$

Conclusions

The problem with this type of analysis is that compromises are necessary which result in a loss of accuracy.

The first difficulty is the overlapping of the diffraction peaks for both monoxides, which necessitates analysis by the use of the peak height at half-peak width instead of the step integration technique. It was shown, however,

that this did not introduce an excessive error, since both methods may be considered equivalent within a 98% confidence level.

Another problem which could not be overcome was the high mass absorption coefficient of the samples when lead is an important component. This would require such small crystallite size that microabsorption problems would arise, in addition to degradation of the data resulting from amorphous surface layers.

There is also the problem of preferred orientations, chemical homogeneity, adequate wavelength, and likely allotropic transformations during grinding.

All these aspects were studied to determine the best conditions and to reduce errors to a minimum.

These precautions allowed measurements of results to be made with comparatively small errors.

The results of the Barton oxides which were analysed were:

	Mass concentration (%)
1-Barton	
o-PbO	10.5 ± 1.6
t-PbO	91.9 ± 5.8
2-Barton	
o-PbO	52.1 ± 1.3
t-PbO	27.1 ± 2.4
Pb	14.6 ± 2.1

Within a 95% confidence margin, the results may be considered as very acceptable. The larger error for the tetragonal oxide is because its concentration is very high and it exceeds the region of the calibration curve for which synthetic samples were prepared.

Acknowledgements

The authors express their thanks to Dr Eng. J. Ruiz for his valuable remarks on the statistical analysis of the results and text, and to Mr F. Gutiérrez Alday for his help in carrying out the calculation programme.

List of symbols

μ^+	Mass absorption coefficient
$\bar{\mu}$	Linear absorption coefficient
t_{max}	Maximum particle size
$\bar{X}$	Arithmetic mean

S	Standard deviation
t	t-Student
μ	Distribution mean
n	Number of measurements
X_0	Given value of the depending variable
$E\|\hat{y}\|$	Estimated value of the depending variable for a given X_0
S_{xy}^2	Sample variance about regression
n	Number of points used for the regression calculation
$(1-\alpha)\cdot 100$	Confidence estimate
P	Probability

References

1 M. Brachet, *3rd Int. Lead Conf., Venice, 1968*, Pergamon Press, Oxford, p. 202.
2 J. R. Pierson, *Electrochem. Technol., 5* (1967) 323.
3 J. R. Dafler, *J. Electrochem. Soc., 124* (1977) 1312.
4 C. F. Yarnell, *J. Electrochem. Soc., 125* (1978) 1934.
5 R. V. Biagetti and M. C. Weeks, *Bell Syst. Tech. J., 49* (1970) 1305.
6 J. Burbank, *Identification and Characterization of Electrochemical Reaction Products by X-Ray Diffraction*, Naval Research Laboratory, Washington, 1967.
7 J. Bermudez, *Métodos de difracción de Rayos-X*, Ediciones Pirámide S.A., Madrid, 1981, p. 306.
8 B. D. Cullity, *Elements of X-Ray Diffraction*, Addison-Wesley, Reading, 1978, p. 408.
9 H. P. Klugg and L. E. Alexander, *X-Ray Diffraction Procedures*, Wiley–Interscience, New York, 1974, p. 533.
10 G. L. Clark and W. P. Tyler, *J. Am. Chem. Soc., 61* (1941) 58.
11 M. Denby, *Power Sources Conf., 31* (1962) 439.
12 G. L. Clark and R. Rowan, *J. Am. Chem. Soc., 63* (1941) 1302.
13 *Powder Diffraction File*, JCPDS International Centre for Diffraction Data, Pennsylvania, 1981.
14 H. P. Klugg and L. E. Alexander, *X-Ray Diffraction Procedures*, Wiley–Interscience, New York, 1974, p. 371.
15 H. P. Klugg and L. E. Alexander, *X-Ray Diffraction Procedures*, Wiley–Interscience, New York, 1974, p. 542.
16 J. B. Doe, personal communication.
17 H. P. Klugg and L. E. Alexander, *X-Ray Diffraction Procedures*, Wiley–Interscience, New York, 1974, p. 373.
18 J. Nývlt, *Industrial Crystallisation from Solutions*, Butterworths, London, 1971, p. 89.
19 R. J. Hill, *J. Power Sources, 9* (1983) 55.
20 C. Kittel, *Introducción a la Física del estado sólido*, Editorial Reverté S.A., Barcelona, 1976, p. 39.
21 J. Bermudez, *Métodos de difracción de Rayos-X*, Ediciones Pirámide S.A., Madrid, 1981, p. 263.
22 J. A. Ingram, *Introductory Statistics*, Cummings Publishing Company, California, 1974.